α-cluster structures above double shell closures via χEFT double-folding potentials

Dong BAI (柏 栋)

School of Physics Science and Engineering, Tongji University

March 10, 2021

Workshop on recent progress in THSR research

Dong Bai and Zhongzhou Ren, *α-cluster structures above double shell closures via double-folding potentials from chiral effective field theory*, Physical Review C, under review (2021).

Dong Bai and Zhongzhou Ren, *Three-body cluster structures in the heaviest α-conjugate nucleus ^{108}Xe* (2021).

Outline

1. Introduction
   - α clustering above double-shell closures
   - Motivation
2. Theoretical Framework
   - χEFT double-folding potentials
   - Two-body cluster model
   - Three-body cluster model
3. Numerical Results
   - Two-body cluster structures in ^{8}Be, $\cdots$, ^{212}Po
   - Three-body cluster structures in ^{108}Xe
4. Summary

Introduction

α clustering above double shell closures

- $2p + 2n +$ doubly magic nucleus
- $4p + 4n +$ doubly magic nucleus

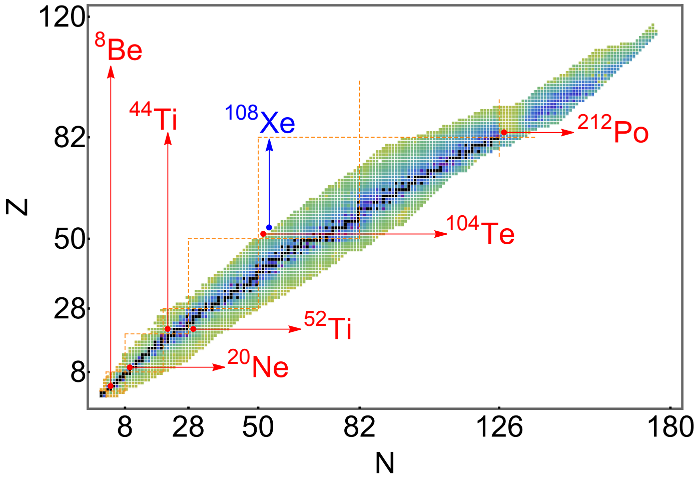

Motivation

- Two-body cluster model $\rightarrow \bigcirc + \alpha$
  - ${}^{8}\mathrm{Be} = \alpha + \alpha,\ {}^{20}\mathrm{Ne} = {}^{16}\mathrm{O} + \alpha, \cdots$
- Three-body cluster model $\rightarrow \bigcirc + \alpha + \alpha$
  - ${}^{108}\mathrm{Xe} = {}^{100}\mathrm{Sn} + \alpha + \alpha$

α-core effective potentials play a crucial role in the two-body and three-body approaches to α-cluster structures outside double shell closures.

1. phenomenological potentials in specific forms
2. double-folding potentials based on effective nucleon-nucleon interactions (M3Y, $\cdots$)

Main Goals

- Construct χEFT double-folding potentials for α + doubly magic nucleus systems
- Study two-body and three-body cluster structures above double shell closures based on χEFT double-folding potentials

Theoretical Framework

χEFT double-folding potentials

Chiral effective field theory (χ**EFT**) is widely regarded as the standard model for nuclear interactions.

- Weinberg, van Kolck, Machleidt, Entem, Meißner, Epelbaum, Forssén, Ekström, Gezerlis, $\cdots$;
- **EFT for nucleons and pions** obeying **chiral symmetry breaking**;
- **Power-counting scheme**
  - ○ Hierarchical structures of 2N, 3N, 4N, $\cdots$ interactions;
  - ○ Systematical improvement;
  - ○ Uncertainty quantification.

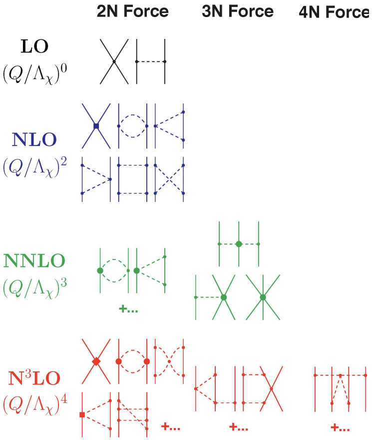

In practice, χEFT gives different realizations of chiral potentials, which are generally **non-local** in coordinate space.

- dependence on $\boldsymbol{k} \equiv (\boldsymbol{p} + \boldsymbol{p}')/2$
- non-local regulator

Local chiral potentials are available up to the **next-to-next-to-leading order** (**N**^{2}**LO**).

A. Gezerlis *et al.*, Phys. Rev. Lett. **111**, 032501 (2013).
A. Gezerlis *et al.*, Phys. Rev. C **90**, 054323 (2014).

At the $\mathrm{N^2LO}$, **local chiral** NN **potentials** are given by

$$
\begin{aligned}
V_{\mathrm{chiral}}(\boldsymbol{r}) &= V_{\mathrm{long}}(\boldsymbol{r})\left\{1-\exp[-(r/R_0)^4]\right\} + V_{\mathrm{short}}(\boldsymbol{r}), \\
V_{\mathrm{long}}(\boldsymbol{r}) &= V_{\mathrm{C}}(r) + W_{\mathrm{C}}(r)\boldsymbol{\tau}_1\cdot\boldsymbol{\tau}_2 + \left[V_{\mathrm{S}}(r) + W_{\mathrm{S}}(r)\boldsymbol{\tau}_1\cdot\boldsymbol{\tau}_2\right]\boldsymbol{\sigma}_1\cdot\boldsymbol{\sigma}_2 \\
&\quad + \left[V_{\mathrm{T}}(r) + W_{\mathrm{T}}(r)\boldsymbol{\tau}_1\cdot\boldsymbol{\tau}_2\right]S_{12}, \\
V_{\mathrm{short}}(\boldsymbol{r}) &= (C_{\mathrm{S}} + C_{\mathrm{T}}\boldsymbol{\sigma}_1\cdot\boldsymbol{\sigma}_2)\,\delta_{R_0}(\boldsymbol{r}) - (C_1 + C_2\boldsymbol{\tau}_1\cdot\boldsymbol{\tau}_2)\Delta\delta_{R_0}(\boldsymbol{r}) \\
&\quad - (C_3 + C_4\boldsymbol{\tau}_1\cdot\boldsymbol{\tau}_2)\,\boldsymbol{\sigma}_1\cdot\boldsymbol{\sigma}_2\Delta\delta_{R_0}(\boldsymbol{r}) + \frac{C_5}{2}\frac{\partial_r\,\delta_{R_0}(\boldsymbol{r})}{r}\boldsymbol{L}\cdot\boldsymbol{S} \\
&\quad + (C_6 + C_7\boldsymbol{\tau}_1\cdot\boldsymbol{\tau}_2) \\
&\quad \times \left\{(\boldsymbol{\sigma}_1\cdot\widehat{\boldsymbol{r}})(\boldsymbol{\sigma}_2\cdot\widehat{\boldsymbol{r}})\left[\frac{\partial_r\,\delta_{R_0}(\boldsymbol{r})}{r} - \partial_r^2\delta_{R_0}(\boldsymbol{r})\right] - \boldsymbol{\sigma}_1\cdot\boldsymbol{\sigma}_2\frac{\partial_r\,\delta_{R_0}(\boldsymbol{r})}{r}\right\}.
\end{aligned}
$$

$\delta_{R_0}(\boldsymbol{r}) = \frac{1}{\pi\Gamma(3/4)R_0^3}\exp[-(r/R_0)^4]$ is the regularized delta function, with R_0 being the **regularization scale** in coordinate space.

The double-folding potential between the α cluster and the core nucleus is given by

$$U_{\mathrm{DF}}(\boldsymbol{R}) = U_{\mathrm{D}}(\boldsymbol{R}) + U_{\mathrm{Ex}}(\boldsymbol{R}),$$

$$U_{\mathrm{D}}(\boldsymbol{R}) = \sum_{i,j=p,n} \int \mathrm{d}^3 r_\alpha \int \mathrm{d}^3 r_C \, \rho_\alpha^i(\boldsymbol{r}_\alpha) V_{\mathrm{D}}^{ij}(\boldsymbol{s}) \, \rho_C^j(\boldsymbol{r}_C),$$

$$U_{\mathrm{Ex}}(\boldsymbol{R}) = \sum_{i,j=p,n} \int \mathrm{d}^3 r_\alpha \int \mathrm{d}^3 r_C \, \rho_\alpha^i(\boldsymbol{r}_\alpha, \boldsymbol{r}_\alpha + \boldsymbol{s}) V_{\mathrm{Ex}}^{ij}(\boldsymbol{s}) \, \rho_C^j(\boldsymbol{r}_C, \boldsymbol{r}_C - \boldsymbol{s})$$

$$\times \exp(i\boldsymbol{k}_{\mathrm{rel}} \cdot \boldsymbol{s}/A_{\mathrm{red}}),$$

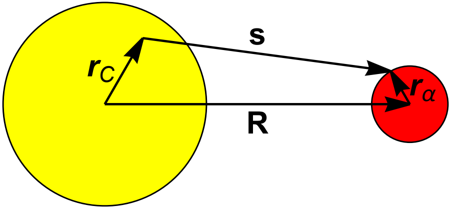

- Model space

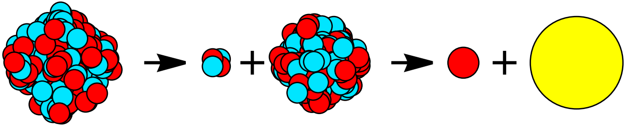

- Wildermuth condition
  - ^{8}Be: $G \equiv 2N + L < 4$ ✗
  - ^{20}Ne: $G < 8$ ✗
  - ^{44}Ti: $G < 12$ ✗
  - ^{52}Ti: $G < 12$, $(G, L) = (12, 12)$ ✗
  - ^{104}Te: $G < 16$, $(G, L) = (14, 16), (16, 16)$ ✗
  - ^{212}Po: $G < 22$, $(G, L) = (22, 20), (22, 22)$ ✗

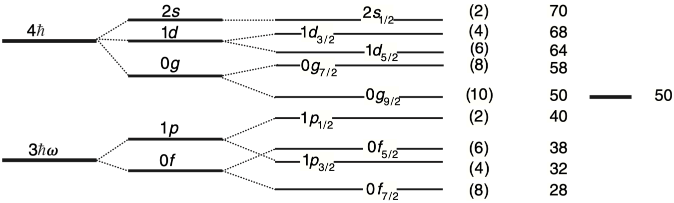

Three-body cluster model

- Model space

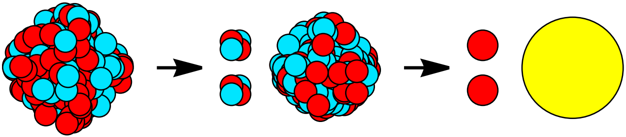

- Hamiltonian

$$H_{3B} = T_{3B} + \int d^3r_1'\, V_{\alpha\alpha}(\boldsymbol{r}_1, \boldsymbol{r}_1') + \int d^3r_2'\, V_{\alpha c}(\boldsymbol{r}_2, \boldsymbol{r}_2') + \int d^3r_3'\, V_{\alpha c}(\boldsymbol{r}_3, \boldsymbol{r}_3') + W_{3B}(\rho),$$

$$V_{\alpha\alpha}(\boldsymbol{r}_1, \boldsymbol{r}_1') = \sum_{LM} \langle \hat{r}_1 | LM \rangle \langle LM | \hat{r}_1' \rangle \left[U_{\alpha\alpha L}(r_1) + U^{\text{rep}}_{\alpha\alpha L}(r_1) \right] \delta(r_1 - r_1')/r_1'^2,$$

$$V_{\alpha c}(\boldsymbol{r}_b, \boldsymbol{r}_b') = \sum_{LM} \langle \hat{r}_b | LM \rangle \langle LM | \hat{r}_b' \rangle \left[U_{\alpha c L}(r_b) + U^{\text{rep}}_{\alpha c L}(r_b) \right] \delta(r_b - r_b')/r_b'^2,$$

$$U_{\alpha\alpha L}(r_1) = U^{\text{Coul}}_{\alpha\alpha}(r_1) + \lambda_{\alpha\alpha L} U^{\text{Nucl}}_{\alpha\alpha}(r_1),$$

$$U_{\alpha c L}(r_b) = U^{\text{Coul}}_{\alpha c}(r_b) + \lambda_{\alpha c L} U^{\text{Nucl}}_{\alpha c}(r_b).$$

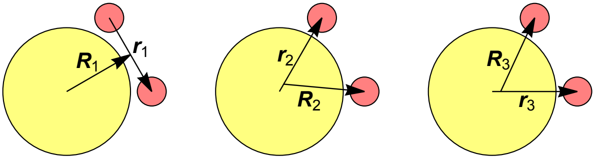

- Stochastic variational method (SVM)

$$\Psi_{3B} = \sum_{i=1}^{M_{\max}} f_i \left[\Phi_{1i}(\boldsymbol{r}_1, \boldsymbol{R}_1) + \overline{\Phi}_{1i}(\boldsymbol{r}_1, \boldsymbol{R}_1)\right] + \sum_{j=1}^{N_{\max}} g_j \left[\Phi_{2j}(\boldsymbol{r}_2, \boldsymbol{R}_2) + \Phi_{2j}(\boldsymbol{r}_3, \boldsymbol{R}_3)\right],$$

$$\Phi_{ak}(\boldsymbol{r}_a, \boldsymbol{R}_a) = \exp(-A_{ak}\, r_a^2 - B_{ak}\, R_a^2 - 2C_{ak}\, \boldsymbol{r}_a \cdot \boldsymbol{R}_a),$$

$$\overline{\Phi}_{ak}(\boldsymbol{r}_a, \boldsymbol{R}_a) = \exp(-A_{ak}\, r_a^2 - B_{ak}\, R_a^2 + 2C_{ak}\, \boldsymbol{r}_a \cdot \boldsymbol{R}_a), \quad (a = 1, 2).$$

Here, $\{A_{ak}, B_{ak}, C_{ak}\}$ are the nonlinear SVM parameters, $\{f_i, g_j\}$ are the linear expansion coefficients, and $\Phi_{ak}(\boldsymbol{r}_a, \boldsymbol{R}_a)$ is the explicitly correlated Gaussian basis function.

Y. Suzuki and K. Varga, *Stochastic Variational Approach to Quantum-Mechanical Few-Body Problems* (Springer, New York, 1998).

Numerical Results

Soft local chiral *NN* potentials

V. Durant, P. Capel, L. Huth, A. B. Balantekin, and A. Schwenk (2018).

- regularization scale R_0=1.6 fm $\rightarrow$ **soft**
- $C_S, C_T, C_1, \cdots, C_7$ determined by fitting Nijmegen *np* phase shifts in $^1S_0$, $^3S_1$, $^1P_1$, $^3P_0$, $^3P_1$, $^3P_2$, and $^3S_1$-$^3D_1$ channels at 1, 5, 10, 25, 50, 100, and 150 MeV.
- deuteron binding energy $E_d = 2.178$ MeV.

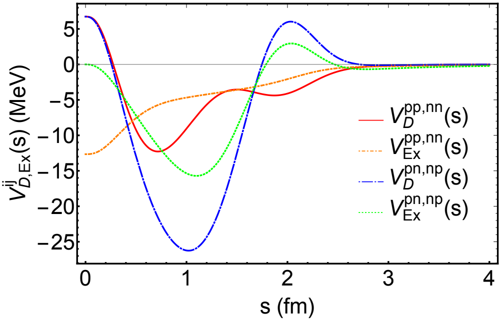

χEFT double-folding potentials for α + doubly magic nucleus systems

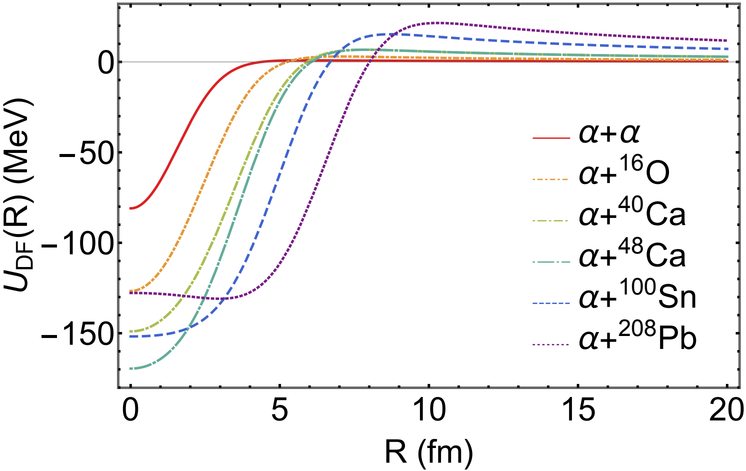

In two-body cluster model,

$$\left[-\frac{\nabla_{\boldsymbol{R}}^2}{2m_{\rm red}} + U(\boldsymbol{R})\right]\Psi_{NLM}(\boldsymbol{R}) = E_{NL}\Psi_{NLM}(\boldsymbol{R}),$$

$$U(\boldsymbol{R}) = \lambda_{NL} U_{\rm DF,N}(\boldsymbol{R}) + U_{\rm DF,C}(\boldsymbol{R}).$$

- ○ λ_{NL}: phenomenological renormalization factor
- ○ $U_{\rm DF,N}(\boldsymbol{R})$: nuclear part of the χEFT double-folding potential
- ○ $U_{\rm DF,C}(\boldsymbol{R})$: Coulomb part of the χEFT double-folding potential

λ_{NL} is determined by reproducing exactly experimental energy of α-cluster state.

- $\Gamma_\alpha \geq 0.01$ MeV $\rightarrow$ complex scaling method (CSM)
- $\Gamma_\alpha < 0.01$ MeV $\rightarrow$ modified two-potential approach/calculable R-matrix theory

$^{8}\mathrm{Be} = \alpha + \alpha$

Nucleus	G	L^{π}	λ_{NL}	$\Gamma_{\alpha}^{\mathrm{exp}}$ [MeV]	Γ_{α}^{χ} [MeV]	$\Gamma_{\alpha}^{\mathrm{NL}}$ [MeV]	R_{rel}^{χ} [fm]
$^{8}\mathrm{Be}$	4	0_1^+	1.4340275	$(5.57 \pm 0.25) \times 10^{-6}$	6.09×10^{-6}	9.8×10^{-6}	5.33
		2_1^+	1.402429	1.513 ± 0.015	1.72	1.33	$2.59 + 0.31i$
		4_1^+	1.46325	≈ 3.5	3.18	4.4	$2.90 + 0.80i$

$^{20}\mathrm{Ne} = \alpha + {}^{16}\mathrm{O}$

Nucleus	G	L^π	λ_{NL}	$\Gamma_\alpha^{\rm exp}$ [MeV]	Γ_α^χ [MeV]	$P_\alpha^{\rm AMD}$	P_α^χ	$P_\alpha^{\rm h}$	$B(\mathrm{E2}\downarrow)_{\rm exp}$	$B(\mathrm{E2}\downarrow)_\chi$ [W.u.]	$B(\mathrm{E2}\downarrow)_{\rm h}$ [W.u.]	$R_{\rm rel}^\chi$ [fm]
^{20}Ne	8	0_1^+	1.1518273			0.70						3.79
		2_1^+	1.1370375			0.68			20.3 ± 1.0	13.0	14.3	3.80
		4_1^+	1.13190728			0.54			22 ± 2	17.1	18.5	3.73
		6_1^+	1.1172209	$(1.1 \pm 0.2)\times10^{-4}$	3.64×10^{-4}	0.34	0.30 ± 0.05	0.19 ± 0.04	20 ± 3	15.2	15.2	3.62
		8_1^+	1.1674842	$(3.5 \pm 1.0)\times10^{-5}$	1.98×10^{-4}	0.28	0.18 ± 0.05	0.095 ± 0.027	9.0 ± 1.3	7.0	7.9	3.21
	9	1_1^-	1.1919326	$(2.8 \pm 0.3)\times10^{-5}$	2.72×10^{-5}	0.95	1.03 ± 0.11	0.82 ± 0.09				4.78
		3_2^-	1.2043384	$(8.2 \pm 0.3)\times10^{-3}$	7.95×10^{-3}	0.93	1.03 ± 0.04	0.67 ± 0.02	50 ± 8	41.6	77.0	4.84
		5_3^-	1.2074985	0.145 ± 0.40	0.114	0.88	1.27 ± 0.35	0.73 ± 0.20		$40.0 + 9.6i$	126.9	$4.52 + 0.30i$
		7_3^-	1.202514	0.110 ± 0.010	0.314	0.71	0.35 ± 0.03	0.20 ± 0.02		$27.8 + 10.7i$	154.9	$4.09 + 0.32i$
		9_5^-	1.18843	0.225 ± 0.040	0.354	0.70	0.64 ± 0.11	0.38 ± 0.07		$14.7 + 6.5i$	36.6	$3.69 + 0.23i$

- 1_1^-, 3_2^-, 5_3^- states almost have pure α-cluster configurations.
- α-formation probabilities extracted by $P_\alpha = \Gamma_\alpha^{\rm exp}/\Gamma_\alpha^{\rm th}$ are generally compatible with AMD.
- Enhancement of $B(\mathrm{E2}\downarrow)_{3_2^- \to 1_1^-}$ is reproduced.

$^{52}\mathrm{Ti} = \alpha + {}^{48}\mathrm{Ca}$

Nucleus	L^π	λ_{NL}	$B(\mathrm{E2}\downarrow)_{\mathrm{exp}}$ [W.u.]	$B(\mathrm{E2}\downarrow)_{\chi}$ [W.u.]	$B(\mathrm{E2}\downarrow)_{\mathrm{WS}^2}$ [W.u.]	R^{χ}_{rel} [fm]
$^{52}\mathrm{Ti}$	0_1^+	0.9656424				4.20
	2_1^+	0.9564093	$7.5^{+0.4}_{-0.3}$	7.1	9.4	4.20
	4_1^+	0.9497294	$9.5^{+1.4}_{-1.1}$	9.6	12.3	4.16
	6_1^+	0.9550252	$8.7^{+0.6}_{-0.5}$	8.8	11.6	4.05
	8_1^+	0.9584199	0.76 ± 0.09	7.1	9.5	3.93
	10_1^+	0.95336506		5.0	6.6	3.80

$^{212}Po = \alpha + {}^{208}Pb$

Nucleus	G	L^π	λ_L	P_α	Γ_α^{th} [MeV]	$\Gamma_\alpha^{th,refined}$ [MeV]	Γ_α^{exp} [MeV]	$B(E2\downarrow)_{th}$ [W.u.]	$B(E2\downarrow)_{exp}$ [W.u.]	$\sqrt{\langle R^2\rangle}_{rel}$ [fm]
^{212}Po	22	0_1^+	1.0459895	0.094	1.62×10^{-14}	1.53×10^{-15}	$(1.53\pm0.01)\times10^{-15}$			6.26
		2_1^+	1.0376702	0.099	4.18×10^{-13}	4.12×10^{-14}		6.3		6.29
		4_1^+	1.031552	0.095	8.13×10^{-13}	7.72×10^{-14}		8.8		6.27
		6_1^+	1.02607	0.085	3.19×10^{-13}	2.72×10^{-14}	$(1.8^{+1.2}_{-0.5})\times10^{-14}$	9.1	3.9 ± 1.1	6.22
		8_1^+	1.020155	0.072	3.97×10^{-14}	2.85×10^{-15}	$(1.9^{+0.4}_{-0.3})\times10^{-15}$	8.7	2.30 ± 0.09	6.15
		10_1^+	1.010274	0.059	7.28×10^{-15}	4.30×10^{-16}		7.9	2.2 ± 0.6	6.09
		12_1^+	0.993857	0.048	5.57×10^{-15}	2.69×10^{-16}		7.1		6.03
		14_1^+	0.982049	0.033	1.34×10^{-16}	4.40×10^{-18}		5.8		5.96
		18_1^+	0.95507	0.0034	3.01×10^{-21}	1.01×10^{-23}	$(1.01^{+0.02}_{-0.01})\times10^{-23}$			5.81

- $P_\alpha(0_1^+) = 0.094$, consistent with $P_\alpha(0_1^+) = 0.1045$ given by quartetting wave function approach
- $P_\alpha(18_1^+) = 0.0034 \rightarrow$ shell-model state

Three-body cluster structures in ^{108}Xe

$$U^{\rm rep}_{\alpha\alpha L}(r_1) = V^{\rm rep}_{\alpha\alpha L}\exp(-\mu^{\rm rep}_{\alpha\alpha L} r_1^2)$$

$$U^{\rm rep}_{\alpha c L}(r_b) = V^{\rm rep}_{\alpha c L}\exp(-\mu^{\rm rep}_{\alpha c L} r_b^2)$$

$$\boldsymbol{Q^{\rm th}_{\alpha} = 5.2\ \mathrm{MeV}}$$

$$\boldsymbol{T^{\rm th}_{1/2,\alpha} = 13.4\ \mathrm{ns}}$$

$$Q^{\rm exp}_{\alpha} = 5.1(2)\ \mathrm{MeV}$$

$$T^{\rm exp}_{1/2} < 18\ \mathrm{ns}$$

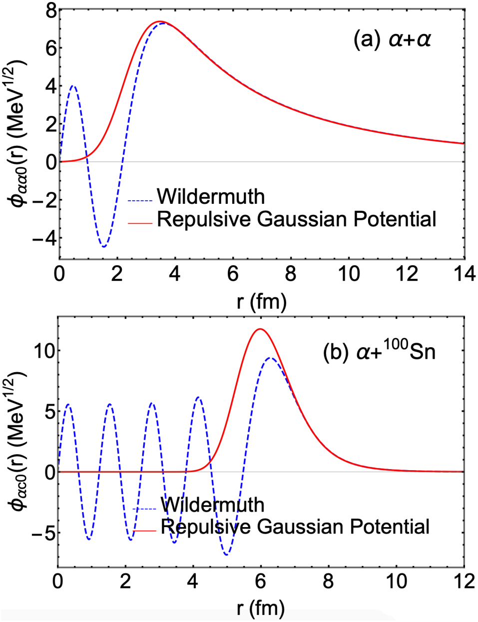

SVM calculations

- without $W_{3B}(\rho)$

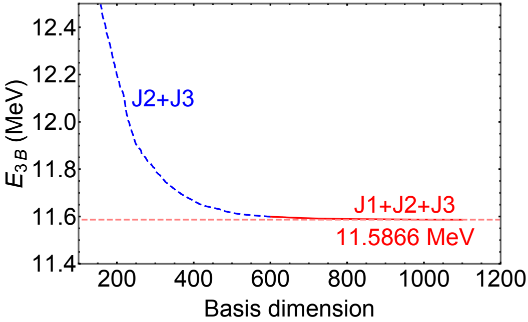

- with $W_{3B}(\rho)$

We take $W = -4.85$ MeV and $\rho_{3B} = 9$ fm. The three-body energy is found to be $E_{3B} = 9.605$ MeV, well consistent with the experimental value ≈ 9.70 MeV.

Density distributions of valence α clusters

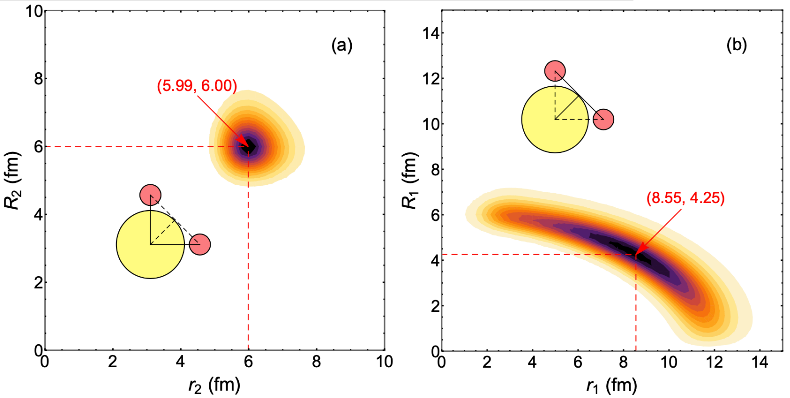

$\sqrt{\langle r_2^2 \rangle} = 6.159$ fm, $\sqrt{\langle R_2^2 \rangle} = 6.155$ fm, $\sqrt{\langle r_1^2 \rangle} = 8.555$ fm, $\sqrt{\langle R_1^2 \rangle} = 4.432$ fm

The relative angle between $\boldsymbol{r}_2$ and $\boldsymbol{R}_2$ is found to be $\theta_2 = \arccos\left(\frac{\langle r_2^2 \rangle + \langle R_2^2 \rangle - \langle r_1^2 \rangle}{2\sqrt{\langle r_2^2 \rangle \langle R_2^2 \rangle}}\right)$ $= 88$ degree ≈ 90 degree.

$\rightarrow$ isosceles right triangle in the ground state of ^{108}Xe

Reduced width amplitudes

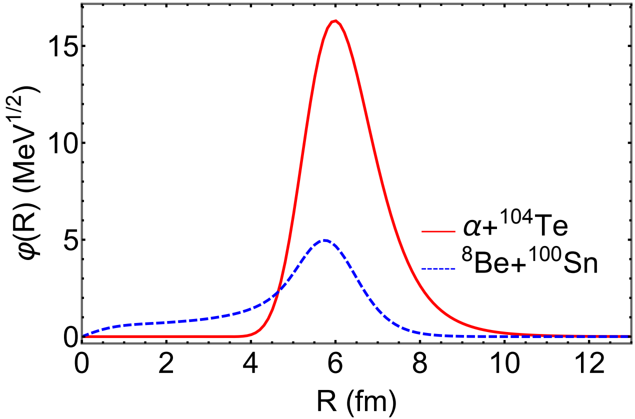

$$\varphi_{\alpha 0}(R_2) = \sqrt{2} R_2 \int \mathrm{d}\hat{R}_2 Y_{00}^*(\hat{R}_2) \int \mathrm{d}^3 r_2\, \phi_{\alpha \mathrm{c} 0}(r_2)/r_2 Y_{00}(\hat{r}_2) \Psi_{3\mathrm{B}}$$

$$\varphi_{\mathrm{Be}0}(R_1) = R_1 \int \mathrm{d}\hat{R}_1 Y_{00}^*(\hat{R}_1) \int \mathrm{d}^3 r_1 \phi_{\alpha\alpha 0}(r_1)/r_2 Y_{00}(\hat{r}_1) \Psi_{3\mathrm{B}}$$

Decay properties of ^{108}Xe

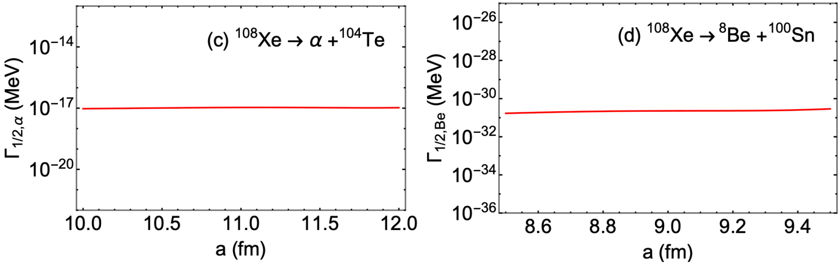

The α-decay half-life of $^{108}\mathrm{Xe} \to \alpha + {}^{104}\mathrm{Te}$ is found to be $T^{\mathrm{th}}_{1/2} \approx 43\ \mu\mathrm{s}$, in good agreement with the experimental value $T^{\mathrm{exp}}_{1/2} = 58^{+106}_{-23}\ \mu\mathrm{s}$. The ^{8}Be-emission half-life is about 2×10^{9} s, larger than the α-decay half-life $T^{\mathrm{th}}_{1/2}$ by thirteen orders of magnitude.

Summary

Summary

- We study two-body and three-body α-cluster structures above double shell closures via χEFT double-folding potentials.
- ^{8}Be, ^{20}Ne, ^{44,52}Ti, ^{104}Te, and ^{212}Po are studied within two-body cluster models to justify χEFT double-folding potentials.
- The heaviest self-conjugate nucleus ^{108}Xe is studied within the three-body cluster model. The α-decay half-life is found to be $T_{1/2}^{\mathrm{th}} \approx 43\ \mu$s, in good agreement with the experimental value $T_{1/2}^{\mathrm{exp}} = 58^{+106}_{-23}\ \mu$s. A novel isosceles right triangular structure made of the two valence α clusters and ^{100}Sn is found in the ground state of ^{108}Xe.

The End

χEFT double-folding potentials

Proton density distributions of α particle, ^{16}O, ^{40,48}Ca, and ^{208}Pb are realistic sums of Gaussians determined in elastic electron scattering experiments, to which **neutron** density distributions are proportional.

H. De Vries, C. W. De Jager, and C. De Vries (1987).

For ^{100}Sn, **São Paulo** distributions are taken

$$\rho^{p,n}(r) = \frac{\rho_0^{p,n}}{1 + \exp\left(\frac{r - R_{p,n}}{a_{p,n}}\right)},$$

with $\mathrm{R_p} = 1.81\mathrm{Z}^{1/3} - 1.12$ fm, $R_n = 1.49N^{1/3} - 0.79$ fm, $a_p = 0.47 - 0.00083Z$ fm, and $a_n = 0.47 + 0.00046N$ fm.

- charge radius $= 4.58$ fm, consistent with $4.525 \sim 4.707$ fm from *ab initio* SCGF + $\mathrm{N^2LO_{sat}}$ chiral potentials.

L. C. Chamon *et al.*, Phys. Rev. C **66**, 014610 (2002).
P. Arthuis, C. Barbieri, M. Vorabbi, and P. Finelli, arXiv:2002.02214.

$\rho^{p,n}_{\alpha(C)}(\boldsymbol{r}_{\alpha(C)}, \boldsymbol{r}_{\alpha(C)} \pm \boldsymbol{s})$ are **density matrix elements** and can be estimated by realistic localization approximation.

D. T. Khoa, W. von Oertzen, and H. G. Bohlen (1994).

$V^{ij}_{\mathrm{D(Ex)}}(\boldsymbol{s})$ is the *NN* interaction in the **direct (exchange)** channel.

For α + doubly magic nucleus, only the central parts of local chiral *NN* potentials make contributions.

$$V^{pp,nn}_{\mathrm{D,Ex}}(s) = \frac{1}{4}\left[V^{01}(s) \pm 3V^{11}(s)\right],$$

$$V^{pn,np}_{\mathrm{D,Ex}}(s) = \frac{1}{8}\left[\pm V^{00}(s) + V^{01}(s) + 3V^{10}(s) \pm 3V^{11}(s)\right],$$

with $V^{ST}(s) \equiv \langle SM_S TM_T | V(s) | SM_S TM_T \rangle$ being the spin-isospin projection of the central parts of local chiral *NN* potentials.

^{44}Ti $= \alpha + {}^{40}$Ca

Nucleus	G	L^π	λ_{NL}	$B(\mathrm{E2}\downarrow)_\chi$ [W.u.]	$B(\mathrm{E2}\downarrow)_{\mathrm{exp}}$ [W.u.]	R^χ_{rel} [fm]
^{44}Ti	12	0^+_1	1.1019607			4.32
		2^+_1	1.0915923	9.9	13 ± 4	4.33
		4^+_1	1.0853305	13.4	30 ± 5	4.28
		6^+_1	1.08476	12.7	17.0 ± 2.4	4.18
		8^+_1	1.078867	10.5		4.06
		10^+_1	1.0990893	6.7		3.85
		12^+_1	1.1338819	3.0		3.63
	13	1^-_2	1.1232387			4.86
		3^-_6	1.116978	20.0		4.83
		5^-_3	1.1053947	22.1		4.78
		7^-_2	1.0972716	20.7		4.67

Benchmark of the SVM code

Positronium negative ion $\mathrm{Ps}^- = e^- + e^- + e^+$

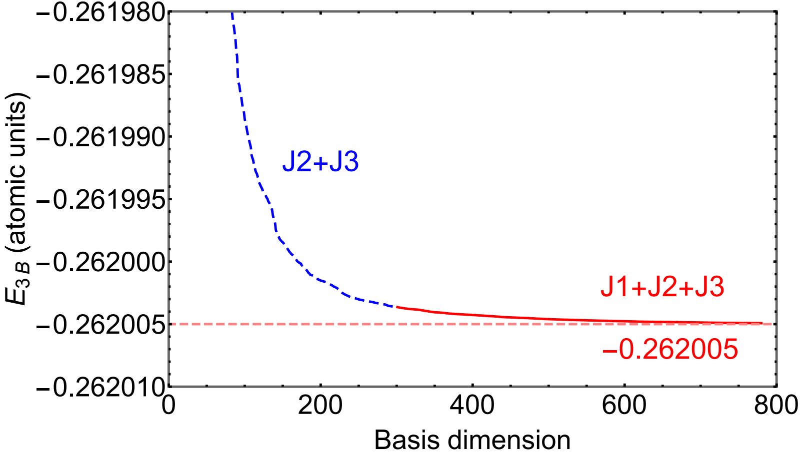

Channel-radius dependence